Supplementary Information

High-performance three-dimensional Ni-Fe layered double hydroxide/graphene electrode for water oxidation†

Xiaowen Yu, Miao Zhang, Wenjing Yuan, and Gaoquan Shi*

Department of chemistry, Tsinghua University, Beijing 100084, People's Republic of China.
E-mail: gshi@tsinghua.edu.cn;
Fax: +86-10-62771149;
Tel: +86-10-62773743

Experimental details

Synthesis of GO

GO was synthesized from natural graphite powder by a modified Hummurs method. 3.0 g of graphite powder (325 mesh) was added to 70 mL concentrated sulfuric acid (98%) under stirring at room temperature. Then, 9.0 g potassium permanganate ($KMnO_4$) was gradually added under vigorous agitation and the temperature of the mixture was kept to be lower than 20 ^oC by ice bath. Successively, the reaction system was stirred at 35 ^oC for 2 h, forming a viscous dark brown mixture. Successively, 500 mL of DI water was added in batches to dilute the mixture and the above system was stirred for another 2 h. Shortly after that, 20 mL of H_2O_2 (30%) was added to neutralize the unreacted $KMnO_4$, turning the color of the mixture from dark brown to yellow. The mixture was filtered and washed by 250 mL HCl aqueous solution (1:10, v/v) to remove metal ions and followed by washing with DI water to remove the acid. The resulting solid was dried in air and diluted to make a GO dispersion (5%, w/w). This dispersion was stirred for one night to make a uniform solution. Finally, it was purified by dialysis using a dialysis membrane with molecular weight cut off of 8000 to 14,000 g mol^{-1} to remove the remaining metal species. After one week, the GO dispersion was centrifuged at 3000 rpm to remove the unoxidized graphite powder and 8000 rpm to concentrate the GO dilute solution.

Supplementary tables

Table S1 Summary of the overpotentials and Tafel slopes of OER at Au, ErGO, Ni-Fe/Au, Ni-Fe/2D-ErGO, and Ni-Fe/3D-ErGO electrodes in an aqueous solution of 1 M KOH.

Electrode	Overpotential (V)	Tafel slope (mV dec^{-1})
Au	0.770	112
3D-ErGO	0.750	100
Ni-Fe/Au	0.331	58
Ni-Fe/2D-ErGO	0.278	42
Ni-Fe/3D-ErGO	0.259	39

Table S2 Summary of overpotentials and Tafel slopes of OER at the Ni-Fe/3D-ErGO electrodes prepared at different potentials applied for depositing Ni-Fe LDH nanoplates.

Deposition potential (V)	Overpotential (V)	Tafel slope (mV dec^{-1})
–1.3	0.274	43
–1.2	0.259	39
–1.1	0.265	43
–1.0	0.268	43
–0.9	0.286	52
–0.8	0.310	49

Table S3 Summary of overpotentials and tafel slopes of OER at the Ni-Fe/3D-ErGO electrodes prepared at −1.2 V from the mixed aqueous solutions of $Ni(NO_3)_2 \cdot 6H_2O$ and $Fe(NO_3)_3 \cdot 9H_2O$ with different Ni/Fe atomic ratios.

Ni/Fe Ratio	Overpotential (V)	Tafel slope (mV dec^{-1})
10:0	0.406	83
9:1	0.271	47
8:2	0.259	39
7:3	0.268	47
6:4	0.266	63
5:5	0.275	47
0:10	0.396	40

Supplementary figures

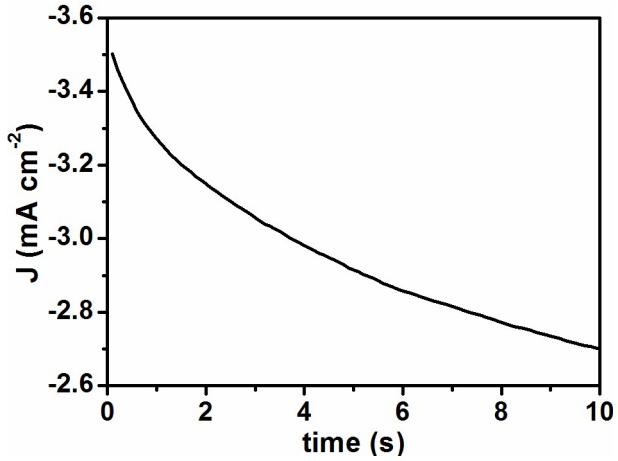

Fig. S1 Current density - time (J - t) curve of Au-RDE in the aqueous solution of 1.6 mg mL^{-1} GO with 0.1 M $LiClO_4$ at a constant potential of −1.0 V.

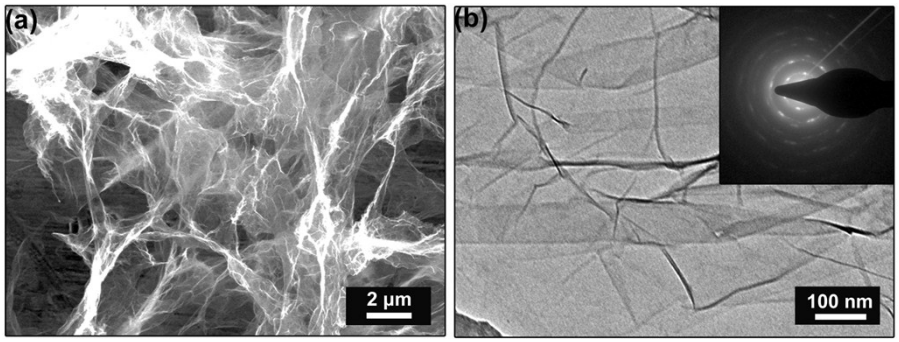

Fig. S2 (a) Top-view SEM image of 3D-ErGO on Au foil with high magnification. (b) TEM image of 3D-ErGO; inset in panel b is the corresponding SAED pattern.

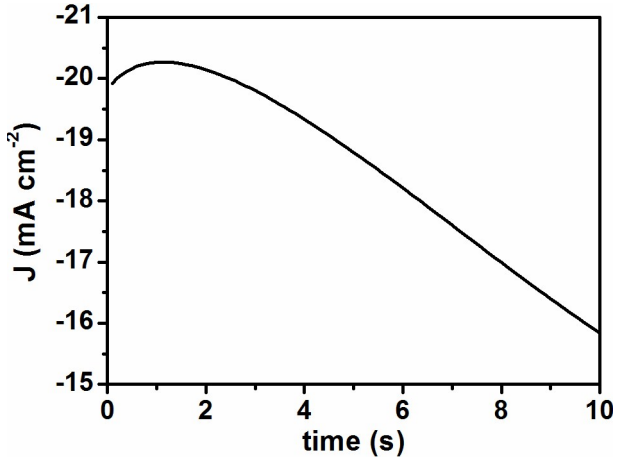

Fig. S3 Current density – time (J - t) curve of 3D-ErGO electrode in a mixed aqueous solution of 40 mM $Ni(NO_3)_2 \cdot 6H_2O$ and 10 mM $Fe(NO_3)_3 \cdot 9H_2O$ at a constant potential of −1.2 V.

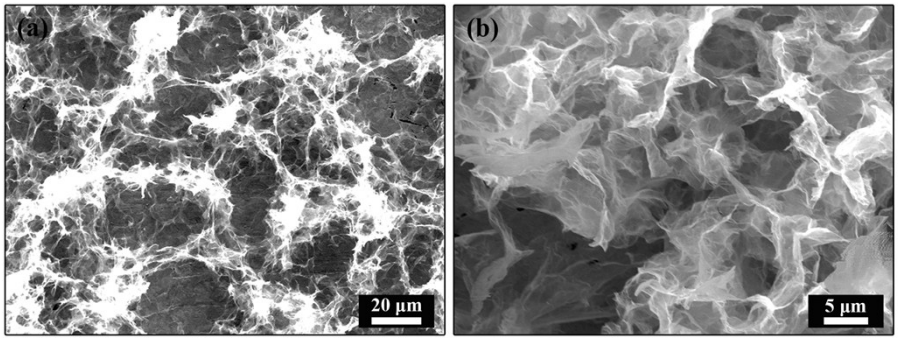

Fig. S4 (a, b) SEM images of Ni-Fe/3D-ErGO with different magnifications.

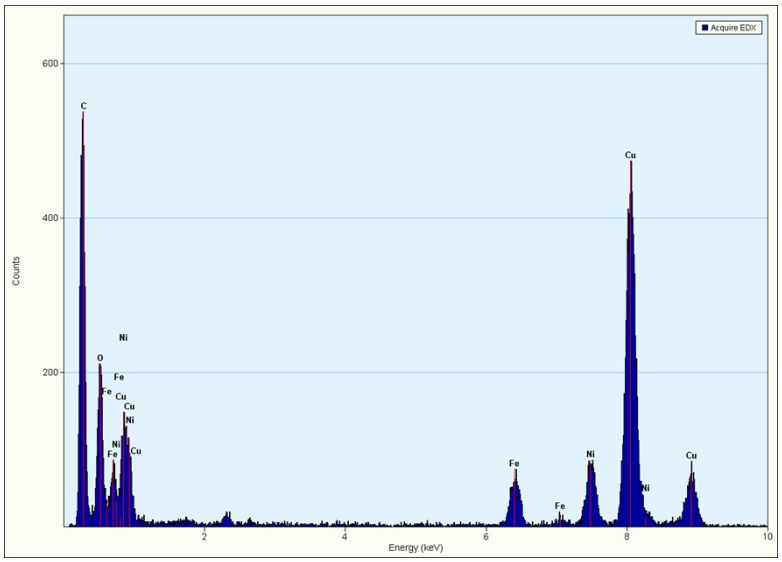

Fig. S5 EDS image of the Ni-Fe/3D-ErGO catalyst shown in Fig. 1e; the signals of Cu are attributed to the copper grid.

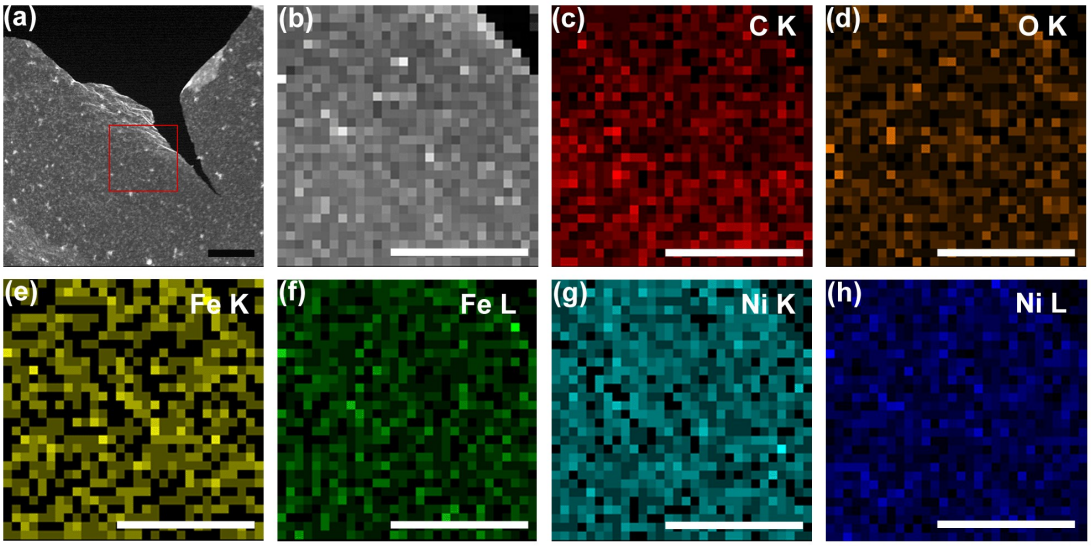

Fig. S6 (a) STEM image of Ni-Fe/3D-ErGO and (b, c, d, e, f, g, h) EDS mapping images of the selected area (red box) shown in panel (a) of all elements (b) and C (c) O (d), Fe (e, f), Ni (g, h) elements. The scale bars = 200 nm.

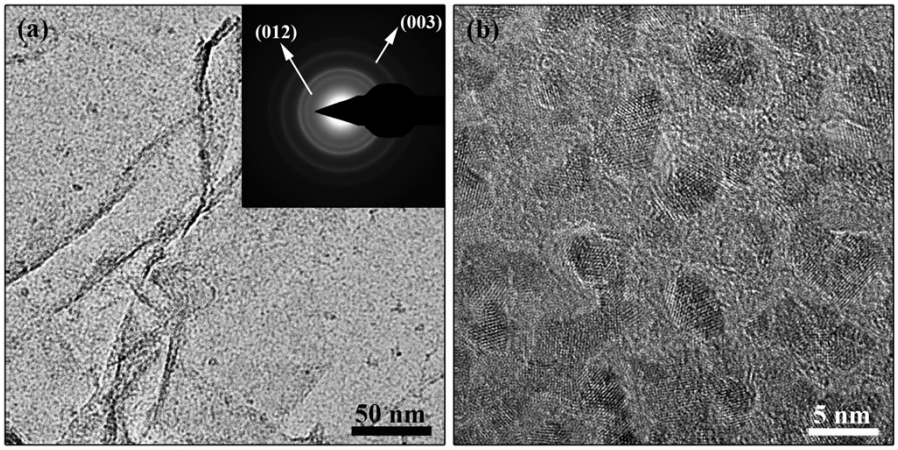

Fig. S7 (a, b) HRTEM images of Ni-Fe/3D-ErGO with different magnifications; inset in panel (a) is the corresponding SAED pattern.

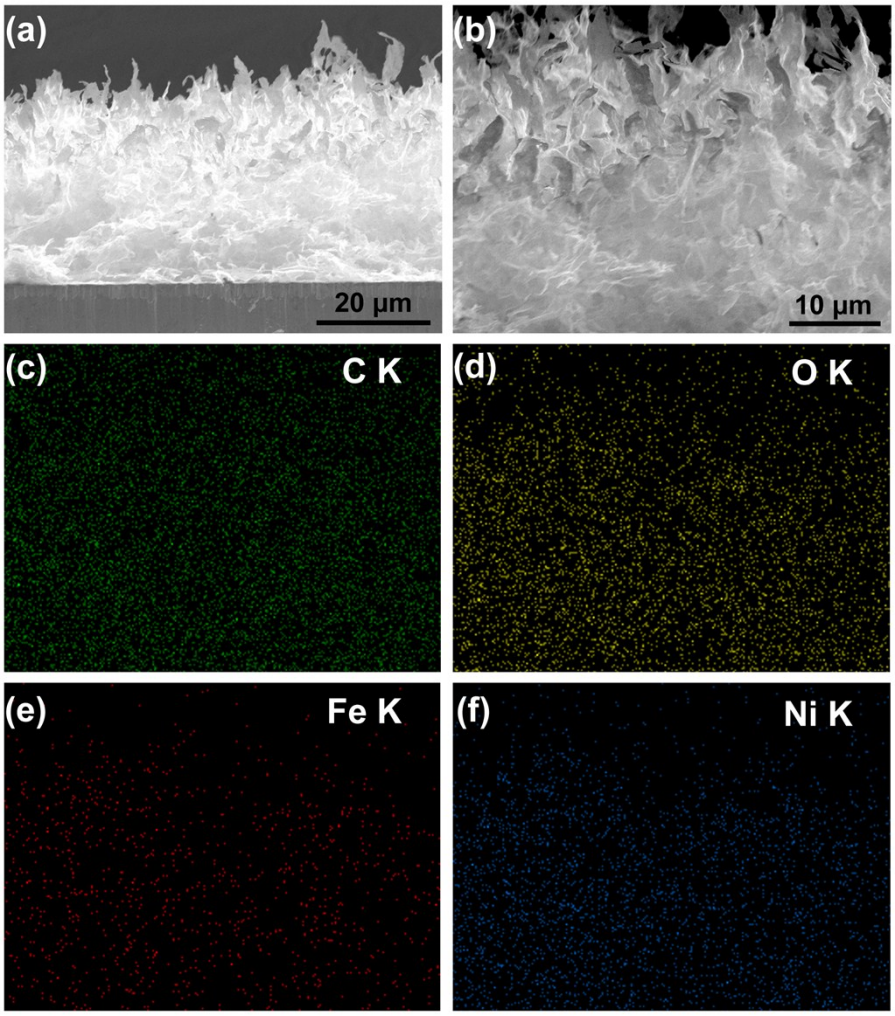

Fig. S8 (a, b) Cross-sectional SEM images of Ni-Fe/3D-ErGO on Au foil with different magnifications. (c, d, e, f) EDS mapping images corresponding to panel (b) of C (c), O (d), Fe (e), and Ni (f) elements.

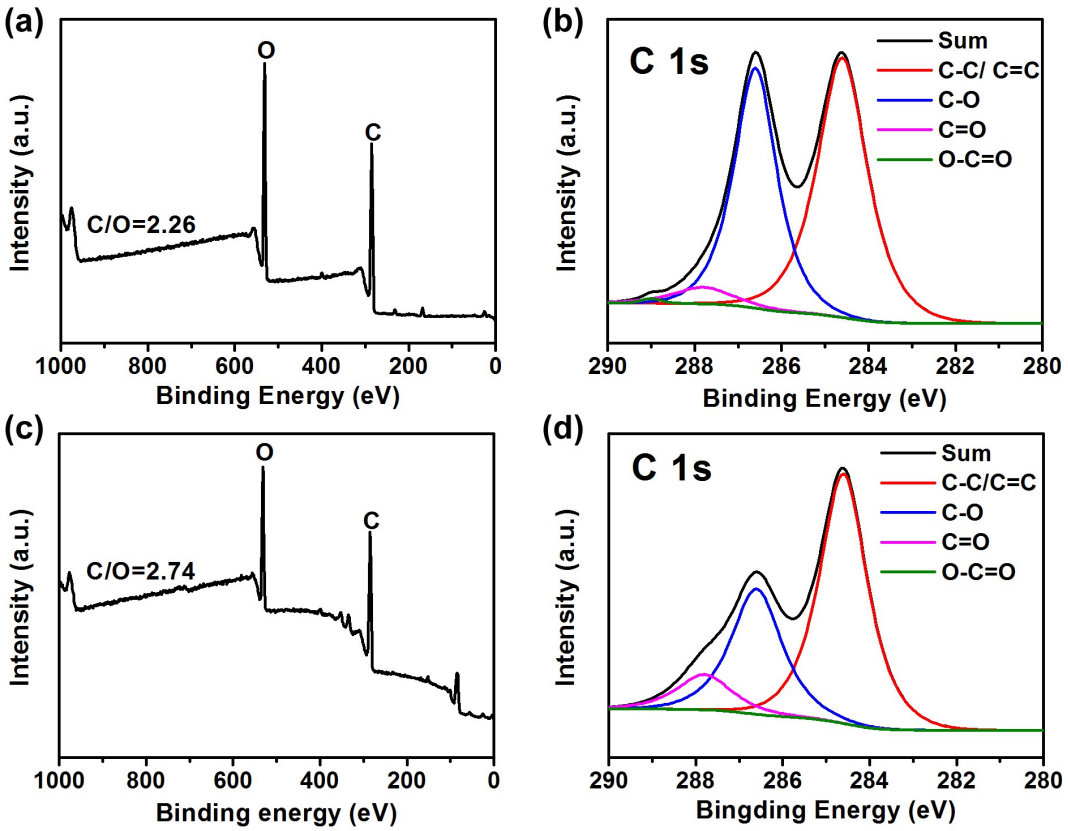

Fig. S9 XPS survey spectra of (a) GO and (c) 3D-ErGO. High-resolution C 1s spectra of (b) GO and (d) 3D-ErGO.

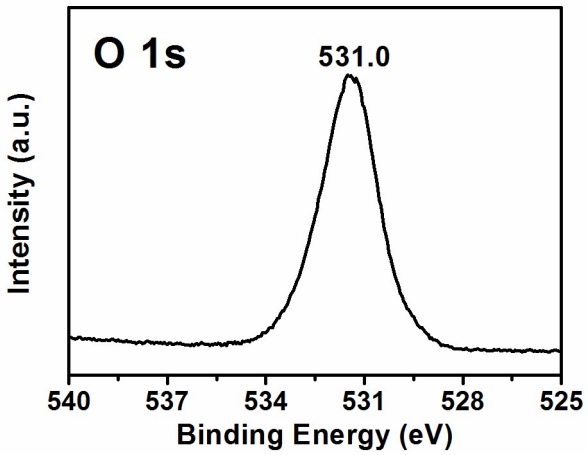

Fig. S10 High-resolution O 1s spectrum of Ni-Fe/3D-ErGO.

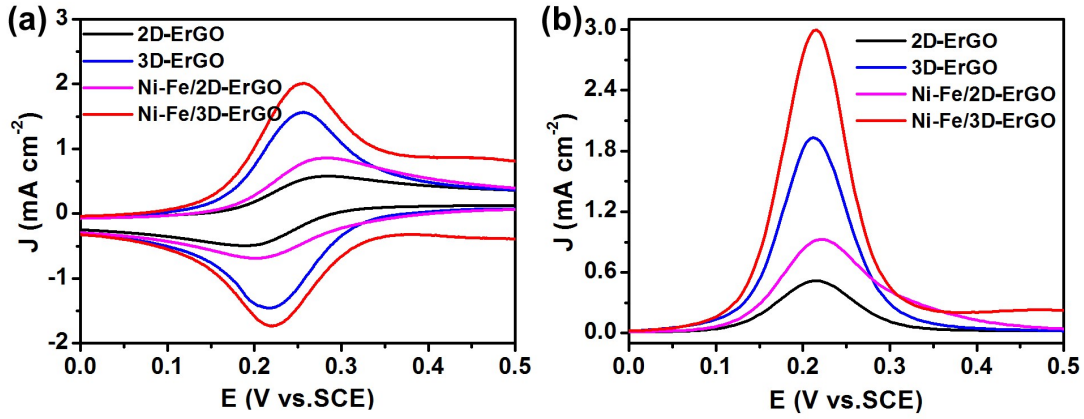

Fig. S11 (a) CVs and (b) DPVs of 2D-ErGO, 3D-ErGO, Ni-Fe/2D-ErGO, and Ni-Fe/3D-ErGO in an aqueous solution of 5 mM $K_4[Fe(CN)_6]$ containing 1 M KCl. The sweep rate for CV curves were 50 mV s^{-1}; the pulse width and period for DPV curves were 0.2 and 0.5 s, respectively.

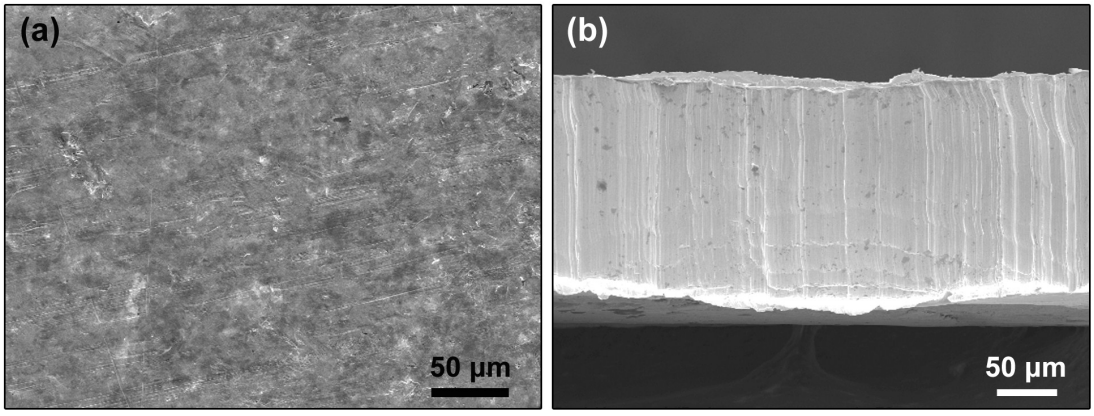

Fig. S12 (a) Top-view and (b) cross-sectional SEM images of 2D-ErGO electrode.

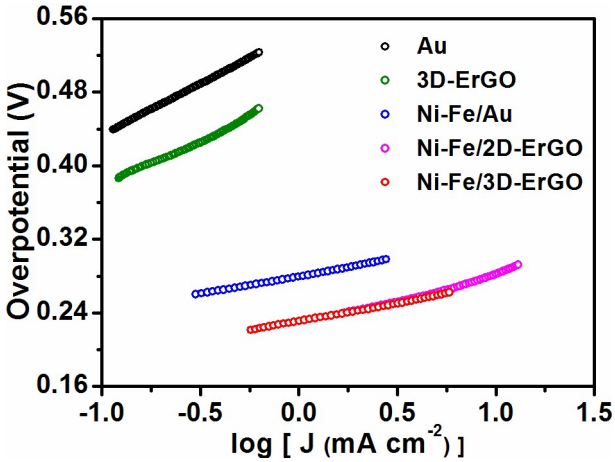

Fig. S13 Tafel plots of Au, 3D-ErGO, Ni-Fe/Au, Ni-Fe/2D-ErGO, and Ni-Fe/3D-ErGO electrodes in the aqueous solution of 1 M KOH.

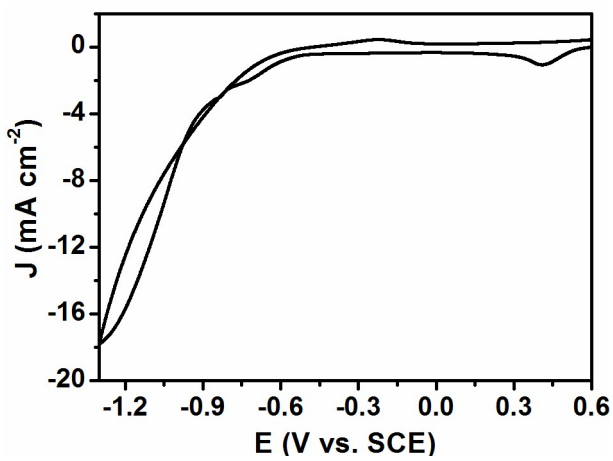

Fig. S14 CV curve of 3D-ErGO electrode in a mixed aqueous solution of 40 mM $Ni(NO_3)_2$•$6H_2O$ and 10 mM $Fe(NO_3)_3$•$9H_2O$. The sweep rate was 50 mV s^{-1}.

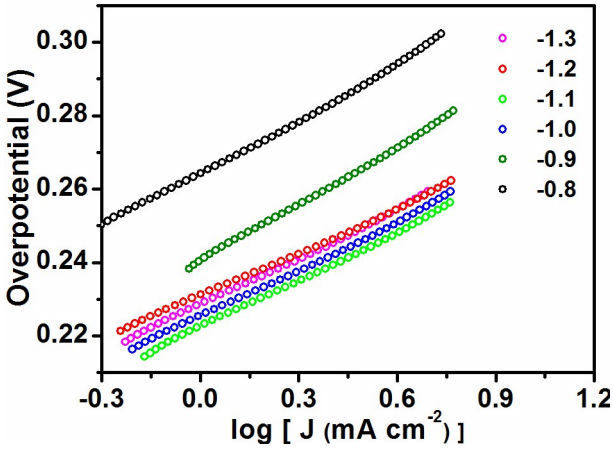

Fig. S15 Tafel plots of different Ni-Fe/3D-ErGO electrodes in the aqueous solution of 1 M KOH; The Ni-Fe/3D-ErGO electrodes were fabricated by depositing Ni-Fe LDH nanoplates at potentials varying from −1.3 to −0.8 V from a mixed aqueous solution of 40 mM $Ni(NO_3)_2$•$6H_2O$ and 10 mM $Fe(NO_3)_3$•$9H_2O$.

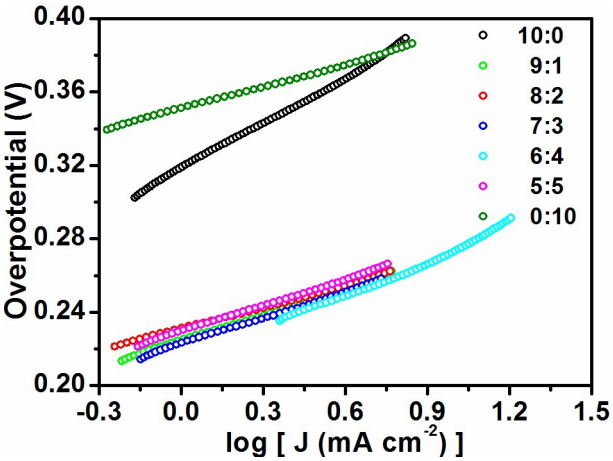

Fig. S16 Tafel plots of different Ni-Fe/3D-ErGO electrodes in the aqueous solution of 1 M KOH; The Ni-Fe/3D-ErGO electrodes were prepared from the Ni-Fe mixed nitrate solutions with Ni/Fe atomic ratio of 10:0, 9:1, 8:2, 7:3, 6:4, 5:5, and 0:10, respectively.

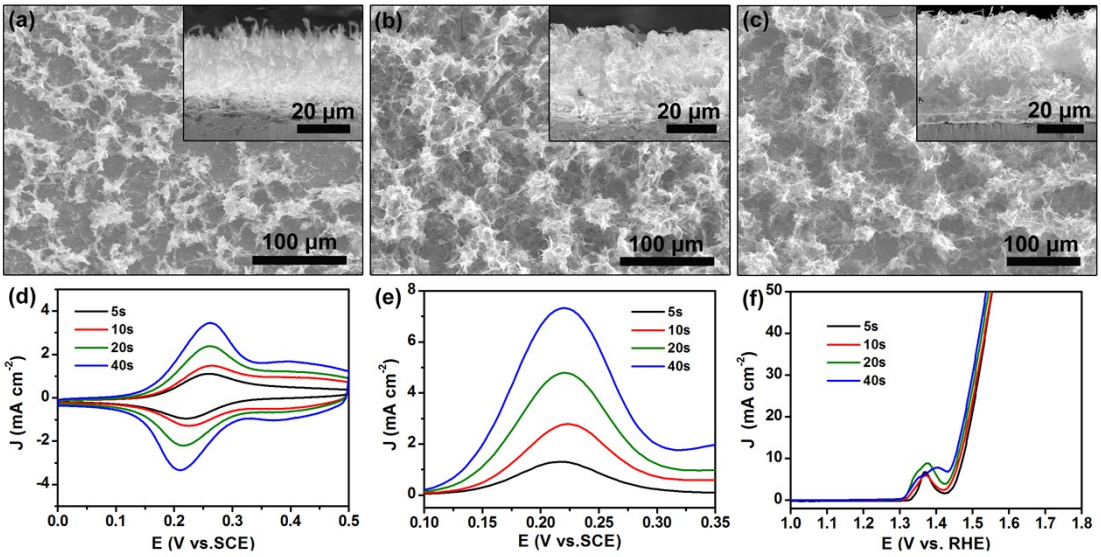

Fig. S17 Top-view SEM images of Ni-Fe/3D-ErGO electrodes prepared with the same Ni-Fe electrodeposition time of 10 s, and the different loading density of ErGO by controlling the electroreduction time of (a) 5 s, (b) 20 s, and (c) 40 s, respectively. Insets are the corresponding cross-sectional SEM images. (d) CV and (e) DPV curves of different Ni-Fe/3D-ErGO electrodes in an aqueous solution of 5 mM $K_4[Fe(CN)_6]$ containing 1 M KCl; scan rate for CV was 50 mV s^{-1}, the pulse width and period for DPV curves were 0.2 and 0.5 s, respectively. (f) LSV curves of Ni-Fe/3D-ErGO electrodes with different loading density of 3D-ErGO; LSV curves were recorded at the scan rate of 10 mV s^{-1} in 1 M KOH.

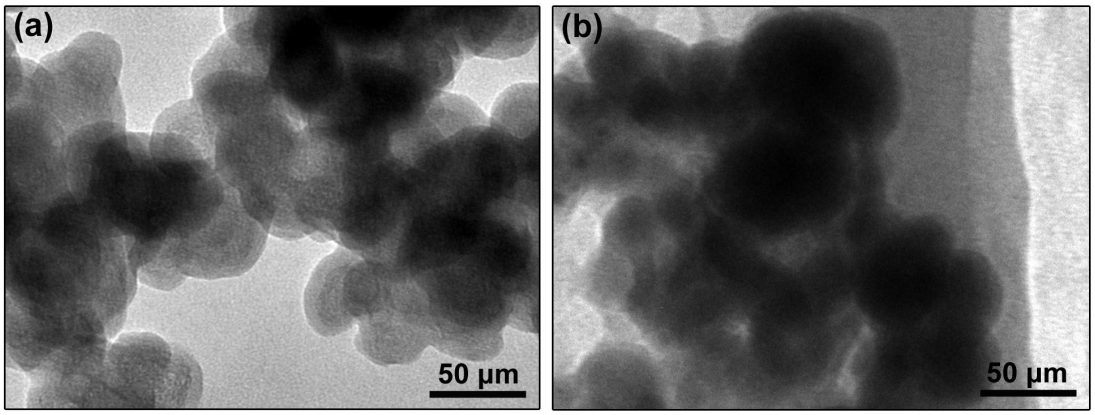

Fig. S18 TEM images of IrO_2 calalyst (a) before and (c) after chronoamperometry test in the aqueous solution of 1 M KOH at a constant potential of 1.70 V for 2 h.

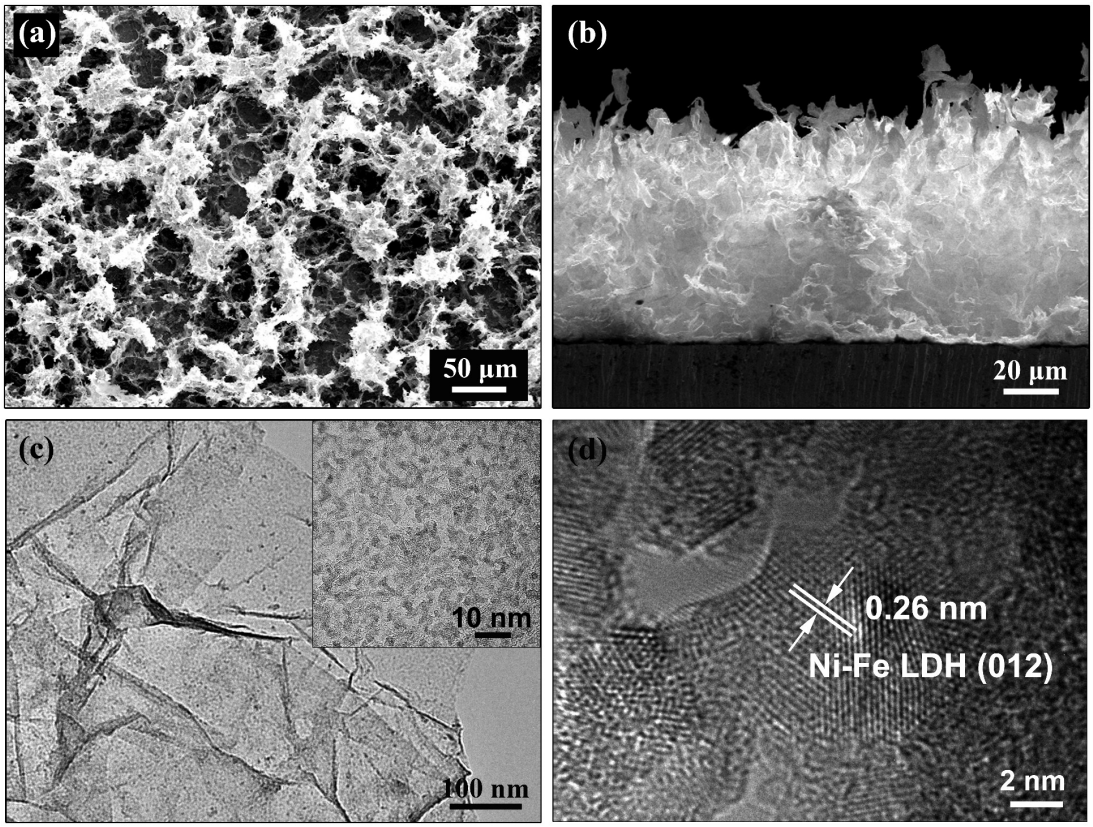

Fig. S19 (a) Top-view and (b) cross-sectional SEM, (c) TEM and (d) HRTEM images of Ni-Fe/3D-ErGO after chronoamperometry test in the aqueous solution of 1 M KOH at a constant potential of 1.49 V for 2 h. Inset of panel (c) is a magnified TEM image.

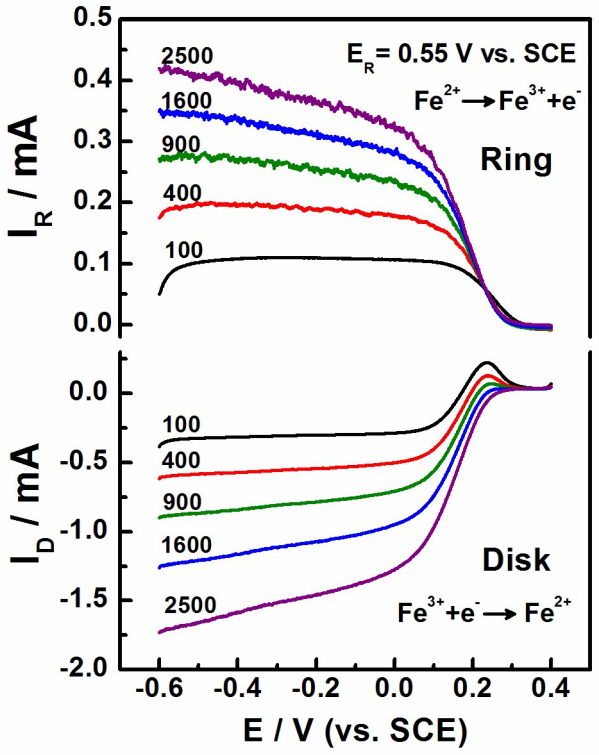

Fig. S20 Curves of ring and disk currents for the calculation of collection efficiency at a Ni-Fe/3D-ErGO RRDE in 0.1 M KOH with 10 mM $K_3Fe(CN)_6$; Sweep rate: 20 mV s^{-1}; Ring electrode was controlled at at a constant potential of 0.55 V (vs. SCE). The RRDE with Ni-Fe/3D-ErGO catalyst on its disk electrode was performed in 0.1 M KOH with 10 mM $K_3Fe(CN)_6$ by LSV. The N was calculated to be 0.29 ± 0.01 using equation of $N = -I_R / I_D$ (the ring (I_R) and disk (I_D) currents in unit of mA).